Annals of Biomedical Engineering, Vol. 37, No. 1, January 2009 *(© 2008)* pp. 129–145
DOI: 10.1007/s10439-008-9594-9

A Mechanobiological Model for Tissue Differentiation that Includes Angiogenesis: A Lattice-Based Modeling Approach

SARA CHECA and PATRICK J. PRENDERGAST

Trinity Centre for Bioengineering, Department of Mechanical & Manufacturing Engineering, School of Engineering, Trinity College, Dublin, Ireland

(Received 23 April 2008; accepted 29 October 2008; published online 15 November 2008)

Abstract—Mechanobiological models have previously been used to predict the time course of the tissue differentiation process, with the local mechanical environment as the regulator of cell activity. However, since the supply of oxygen and nutrients to cells is also a regulator of cell differentiation and oxygen diffusion is limited to few hundred micrometers from capillaries, the morphology of the new vascular network may also play a critical role in the process. In this paper, a computational model for tissue differentiation based on the local mechanical environment and the local vascularity is presented. A regular lattice is used to simulate cell activity (migration, proliferation, differentiation, apoptosis, and angiogenesis). The algorithm for capillary network formation includes mechanoregulation of vessel growth. A simulation of tissue differentiation in a bone/implant gap under shear was performed. The model predicts capillary networks similar to those found in experimental studies and heterogeneous patterns of tissue differentiation, which are influenced by the morphology of the capillary network. Higher mechanical loads caused slower vascular development and delayed bone tissue formations.

Keywords—Blood vessel, Bone/implant interface, Osseointegration, Mechanobiology, Mechanoregulation, Capillary.

INTRODUCTION

The intimate connection between blood vessels and bone formation has long been recognized. According to Trueta,[61] as early as 1763 Albrecht von Haller had suggested that the vascular system is responsible for bone formation[25] stating that 'the origin of bone is the artery carrying the blood and in it the mineral elements'. At this time, the role of osteoblasts in bone formation attracted most of the attention and it was not until 1963 that interest in the vascularity was revised when Trueta suggested the existence of a 'vascular stimulating factor (VSF)' at the sites of bone damage.[61]

Following damage to bone tissues, blood vessels are disrupted and a hematoma is formed. Stem cells are then recruited to the site and new blood vessels are formed from pre-existing ones through the migration and proliferation of endothelial cells in a process known as angiogenesis. Essentially, upon angiogenic stimulation, vascular endothelial cells are activated and begin to degrade their surrounding vessel membrane. Then the endothelial cells migrate into the interstitium, resulting in the formation of capillary sprouts. Endothelial cells behind the migrating endothelium of the sprouts proliferate so that the newly developing blood vessel elongates guided by a chemotactic response to growth factors[60] and a persistence in the direction of growth.[57] Osteogenesis then takes place near newly formed vessels, which mediate delivery of osteoprogenitor cells, secrete mitogens for osteoblasts, and transport nutrients and oxygen.[13] Osteogenic precursor cells in regions of poor vascularity have been shown to follow a chondrogenic rather than an osteogenic pathway.[27,33] In addition, inhibition of new blood vessel formation has been shown to prevent fracture healing in rats[26] while exogenous application of vascular endothelial growth factor (VEGF) has been shown to significantly accelerate fracture healing.[20]

The mechanical environment plays a fundamental role both in the tissue differentiation process and in the development of the new vasculature. Instability in the fracture healing zone has been shown to prevent vascularization and to lead to fibrocartilagenous tissue in the fracture gap,[14,15] while an appropriate load to the fracture site has been shown to promote angiogenesis and osteogenesis.[62] Similarly, long-term clinical success of bone implants, such as knee or hip replacements, require an initial stable anchoring at the bone/implant interface.[58] To allow early blood vessel growth and eventually new bone formation, initial stability has to

Address correspondence to Dr. Sara Checa, Trinity Centre for Bioengineering, Department of Mechanical & Manufacturing Engineering, School of Engineering, Trinity College, Dublin, Ireland. Electronic mail: s.checa@tcd.ie

be achieved by reduction of micromotion.[52] If micromotion cannot be reduced to a minimum level, a fibrous tissue rather than a bony interface will result at the implant surface leading to loosing of the prosthesis.[4,6,8] Control of blood vessel formation and tissue differentiation at the implant surface are therefore important for bone/implant integration and long-term implant stability. Furthermore, angiogenesis is critical for the success of bone tissue engineering where capillary invasion is required before bone formation will occur.

Several mechanoregulation theories have been developed relating mechanical loads and tissue differentiation which have been implemented in computer models to successfully reproduce some of the main aspects of the bone regeneration process.[47] Shear strain, hydrostatic pressure, tensile strain, compressive strain, and fluid flow have all been proposed to regulate the cell differentiation pathway. Based on the level of the mechanical stimulus, mesenchymal stem cells are assumed to differentiate toward fibroblasts, chondrocytes, or osteoblasts, which will synthesize fibrous connective tissue, cartilage, or bone, respectively. Two different approaches have been followed in the development of these models. In the earliest approaches, models were developed to correlate tissue phenotype at specific time points in the fracture healing process with calculated mechanical fields (stress, strain, hydrostatic stress, octahedral shear stress). By relating contour plots to the observed tissue distribution, several mechanoregulation theories were proposed.[5,12,16,56] The second approach uses an iterative procedure to simulate the tissue differentiation process regulated by the local mechanical environment. In each iteration, the mechanical environment is determined from a finite element model. Local magnitudes are then input into a mechanoregulation algorithm which predicts the new tissue phenotype. Changes in the material properties due to the differentiation process are then updated in the finite element model. This approach has been applied to fracture healing,[2,32,38] osteochondral defect healing,[35] distraction osteogenesis,[30,44] tissue engineering,[10,36] and bone ingrowth in bone/implant interfaces.[22,29,40]

None of the above-mentioned computer simulations consider the effect of vascular supply in the process of bone formation; instead they consider the local mechanical environment as the only regulator of tissue differentiation. In an attempt to predict the regeneration process of trabecular bone, Shefelbine *et al.*[53] developed a model for tissue differentiation that included both the local mechanical environment and the amount of vascularization surrounding the regenerating tissue. Assuming a maximum vascularity in all the regenerating tissue at the beginning of the simulation, vascular development was driven by the mechanical environment. However, the mechanical conditions were such that the vascularity stayed maximal throughout the simulation and therefore the effect of oxygen supply on bone formation was not predicted. Using angiogenic factor concentration as a measure of vascularity, Geris *et al.*[23] developed a mathematical model for tissue differentiation to simulate fracture healing. They looked at cell density and growth factor concentration as continuum variables that evolve according to a set of reaction–diffusion equations. Although this model took account of endothelial cell distribution and was therefore a definite advance on previous approaches, it is unable to provide more detailed information concerning the structure and morphology of the capillary network; furthermore, angiogenesis occurred independently of the local level of biophysical stimuli. Since oxygen diffusion is limited to few hundred micrometers from blood vessels[11] and osteogenesis only takes place in well-vascularized environments, the morphology of the newly developed vasculature may play a fundamental role during tissue repair.

In pursuit of a better understanding of the tissue regeneration process, we combined the mechanoregulation algorithm for tissue differentiation proposed by Prendergast *et al.*[46] with a stochastic model for cell migration and proliferation based on random walk theory[48] to simulate capillary network formation and tissue regeneration. Our hypothesis is that capillary network dynamics influences osteogenesis. We tested this hypothesis in a model of a bone/implant interface under shear, where the effect of vascularity-related parameters on simulation predictions was also investigated. If the hypothesis is confirmed, it would suggest that mechanobiological simulations of the tissue regeneration process could be improved with the incorporation of the effect of oxygen supply by the vascular network. Such an advance may facilitate the application of mechanobiological computer simulations in bone tissue engineering.

MATERIAL AND METHODS

The Tissue Differentiation Algorithm

A lattice model was used for the simulation of cell activity. The tissue regeneration domain was divided into a series of lattice points which represent a space for both the cell and the extracellular matrix (Fig. 1). In these lattice points cells migrate, proliferate, and differentiate following a set of rules.

Cell Proliferation

In the model, a cell is surrounded by six lattice points (3D) that a daughter cell can occupy. After

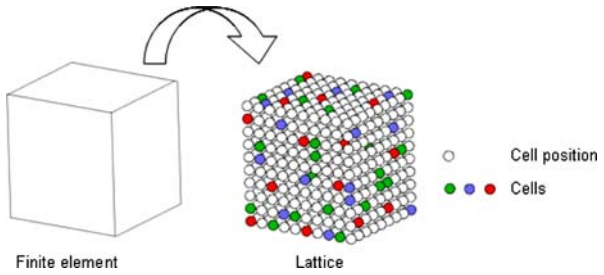

FIGURE 1. Lattice model for the simulation of cell activity. Each lattice point represents a possible position for a cell.

mitosis, two new positions are selected at random. If a selected position is already occupied then another position is selected at random. This process continues until either both cells are placed or all the positions are occupied. In the latter case mitosis does not occur (contact inhibition).

Cell Migration

To model cell migration, a new position is chosen randomly from the surrounding locations. If the selected position is already occupied, a new neighboring position is chosen, again randomly. If there are no free neighboring lattice points then migration ceases. In that case, the cell remains in its original location. Recognizing that cell migration is a more rapid process than cell proliferation, a new location for the migrating cell may be chosen several times during one proliferation cycle.

Cell Differentiation

According to the mechanoregulation algorithm proposed by Prendergast *et al.*[46] precursor cells differentiate based on a combination of two mechanical stimuli, shear strain (γ) and fluid/solid velocity (υ), according to the following equation:

$$S = \frac{\gamma}{a} + \frac{\upsilon}{b},$$

where $a = 0.0375$, $b = 3$ μm/s,[29] and S is a mechanoregulatory stimulus. At high mechanical stimuli, the algorithm predicts mesenchymal stem cell differentiation toward fibroblasts, a medium level of stimuli predicts cell differentiation toward chondrocytes, while at low mechanical stimuli mesenchymal stems cells are predicted to differentiate toward osteoblasts. In the present paper, we extend this to include the effect of vascularity on the tissue differentiation process considering that at low mechanical stimuli cartilage instead of bone will form if there are no blood vessels within a distance from the differentiating cell. This can be expressed as:

IF ($S =$ '*bone*' AND O_2 *low*) THEN
Cartilage formation
IF ($S =$ '*bone*' AND O_2 *high*) THEN
Bone formation

where no blood vessels surrounding the differentiating cell translates into low oxygen concentration (O_2 *low*), while capillaries in the vicinity of the differentiating cell translates into high oxygen concentration (O_2 *high*).

Algorithms for each cellular event (differentiation, angiogenesis, migration, etc.) were combined and implemented to create a simulation of the tissue differentiation process. The simulation begins with a finite element analysis of the domain on which a lattice of potential cell positions has been superimposed. Stems cells and differentiated cells react to the mechanical stimuli and to the presence of oxygen by migration, proliferation, and differentiation while simultaneously a capillary network grows within the same lattice. The growth of the capillaries is also mechanoregulated as described in section "Simulation of Angiogenesis". The time course is simulated as an iterative process (Fig. 2). In each iteration, within each element of the finite element model, a percentage of the mesenchymal stem cells (MSCs) that have reached the maturation age will differentiate toward fibroblasts, chondrocytes, or osteoblasts. When MSCs differentiate a new tissue phenotype is predicted and the material properties at each lattice point inside the element are updated. When the stimulus in an element changes such that a cell type is under an inappropriate mechanical stimulus, cells are removed by apoptosis. A rule of mixtures was used to calculate material properties when two or more different tissue phenotypes exist simultaneously in an element. Instantaneous changes of tissue type in an element were prevented by averaging the material properties from the ten previous iterations.

Simulation of Angiogenesis

The growth of the vascular network was modeled through the following fundamental events:

1. The formation of vessel sprouts from pre-existing sprouts or vessels (branching)
2. The growth of the sprouts
3. The fusion of a sprout tip to another sprout tip or another sprout (anastomosis)

Each capillary was modeled as a sequence of endothelial cells whose path was determined by the path of the endothelial cell at the capillary tip which moved following a random walk with the possibility of directional bias and persistence.

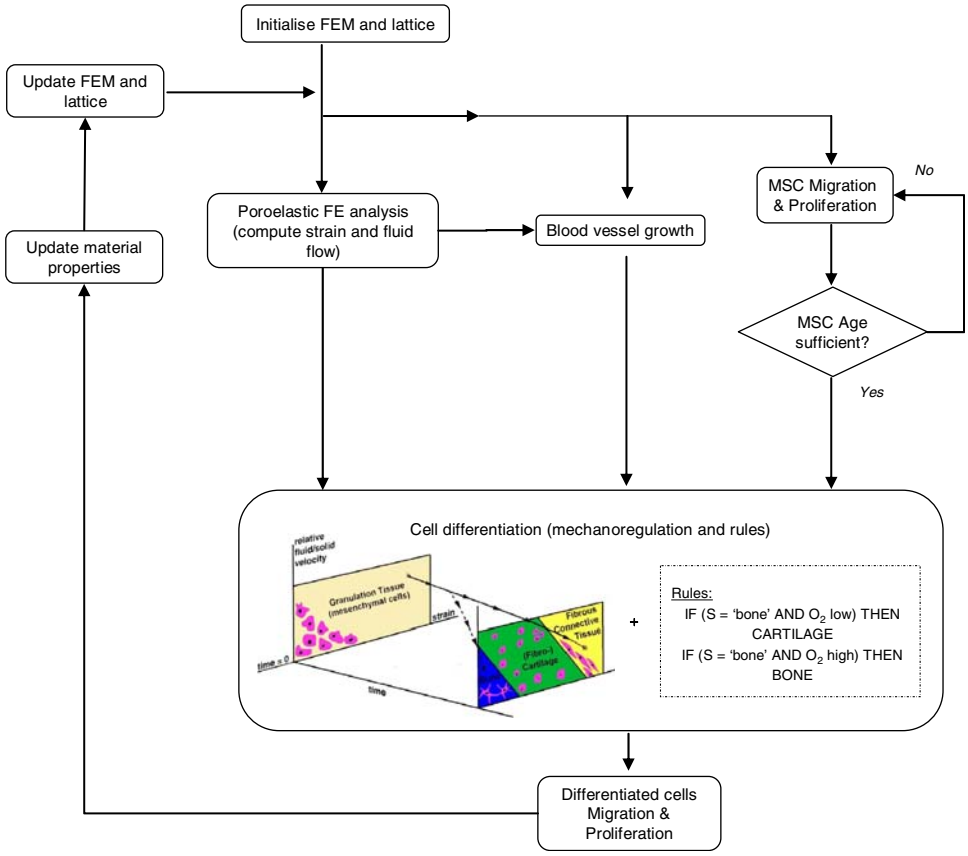

FIGURE 2. Schematic representation of the computational algorithm to model tissue regeneration. The differentiation process is regulated by the local mechanical environment and the local vascularity.

Chemotaxis (directed movement along chemical concentration gradients) was modeled assigning biased probabilities to the 17 possible directions that a tip cell can take (Fig. 3) according to the relative concentration of hypertrophic chondrocytes (mature chondrocytes under a mechanical stimulus favorable for bone formation) in each of the directions, so that the cell is more likely to move toward higher concentrations of hypertrophic chondrocytes. This aims to replicate experimental observations during endochondral ossification where chondrocytes exit their proliferative cycle and mature toward hypertrophic chondrocytes.[50] Hypertrophic chondrocytes in the matrix start producing VEGF, attracting endothelial cells into the mineralized matrix, increasing vascularity and triggering matrix metalloproteinases (MMPs) to degrade the cartilage matrix.[17,21] The direction of growth is then determined based on assigned probabilities for the cell to follow the chemotactic direction (chemotactic direction ratio: p_1), its direction on the previous time step (persistence ratio: p_2), or a random direction (random direction ratio: p_3), such that $p_1 + p_2 + p_3 = 1$.

Sprout formation was modeled as a stochastic process where the probability of a sprout to form from a vessel segment is proportional to the segment length (Fig. 4a). $L_{\min}$ represents the minimum length for a sprout to branch, while $L_{\max}$ represents the maximum length for a nonbranching sprout.

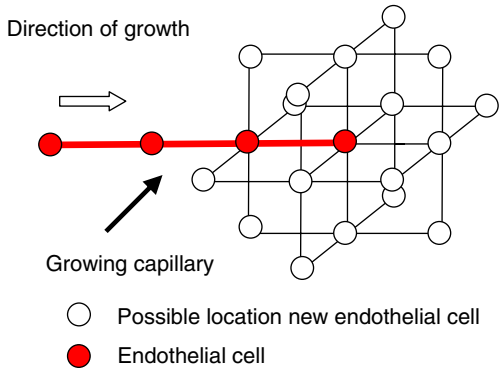

FIGURE 3. Possible directions for endothelial cell migration. The tip cell of a growing capillary is allowed to move to any of the positions represented.

To account for the inhibition of capillary growth into areas of high mechanical environment, we

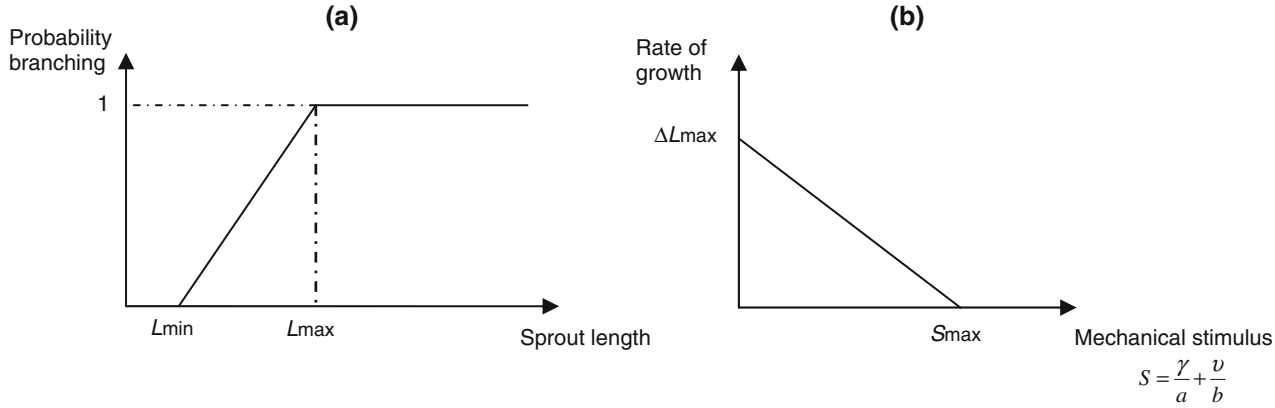

FIGURE 4. (a) Probability of sprout branching as a function of sprout length. L_{min} represents the minimum length for a sprout to branch, while L_{max} represents the maximum length for a nonbranching sprout and (b) Sprout rate of growth as a function of the mechanical stimulus (combination of fluid flow and shear strain).

assumed that the rate of growth is regulated by the local mechanical stimulus such that a high combination of fluid flow and shear strain will prevent capillary vessels from forming (Fig. 4b).

We assumed that if a leading endothelial cell attempts to cross the path of another sprout, or its own path, then anastomosis occurs. The colliding cell ceases to migrate and the capillaries form a closed loop.

A summary of the algorithm for the simulation of angiogenesis is shown in Fig. 5.

Implementation in Osseointegration at a Bone/Implant Interface

The 3D simulation domain corresponds to the gap tissue in a model of a bone/implant interface which includes a bone and an implant layer and the interfacial gap of regenerating tissue (Fig. 6). Poroelastic elements were used for the bone and the gap tissue. Pore pressure and nodal displacements on the upper and lower faces were constrained to be equal to approximate a repeating unit of a long implant *in situ*. Simulations were performed under force-control and displacement-control conditions. Under force-control conditions, the same shear load was applied throughout the simulation; the consequence of this is that the displacement reduces as the tissue stiffens. The magnitude of the load applied was such that the initial relative displacement between the bone and the implant surface was approximately 117 or 233 μm.[9,58] Under displacement-control, a relative displacement between the bone and the implant of 100 μm was maintained throughout the simulation. In this case, the load needed to keep the required displacement increases as the tissue stiffens.

The bone surrounding the gap was assumed properties of cortical bone and the implant was modeled as homogeneous, isotropic, and linear elastic with an elastic modulus of 100 GPa and a Poisson's ratio of 0.3. Table 1 lists the mechanical properties considered for the different tissue phenotypes. It was assumed that the vascular tissues do not contribute to the mechanical stiffness of the system due to their small size and their low mechanical properties. Therefore, material properties were not assigned to the developing vasculature.

To model cell activity, a 3D lattice was created with a distance between lattice points of 0.01 mm. This assumes an average cell diameter of 10 μm for all cell types.[39] Initially, the domain was filled with granulation tissue and a random distribution of MSCs inside the domain was considered (1% of the maximum concentration of cells[48]). Only MSCs and fibroblasts were assumed to migrate, as they are more motile during tissue differentiation than other cell types (osteoblasts and chondrocytes). Five random jumps were performed for each MSC and fibroblast in each iteration of the tissue differentiation simulation.[48] Other cells types dispersed by proliferation only. One proliferation cycle was assumed per cell for each iteration.[48] In each iteration, within each element, 30% of the MSCs that have reached a maturation age (6 iterations[48]) selected at random, differentiated toward fibroblasts, chondrocytes, or osteoblasts depending on the mechanoregulatory stimulus S and the local vascularity. A high concentration of oxygen was assumed within a distance, $L_{diffusion}$, from any blood vessel, while any position further was considered to have low concentration of oxygen. Mature chondrocytes (maturity was assumed after the chondrocyte existed for 6 iterations) under a mechanical stimulus favorable for bone formation were assumed to hypertrophy and express VEGF. Fibroblasts, chondrocytes, or osteoblasts under an unfavorable mechanical stimulus were

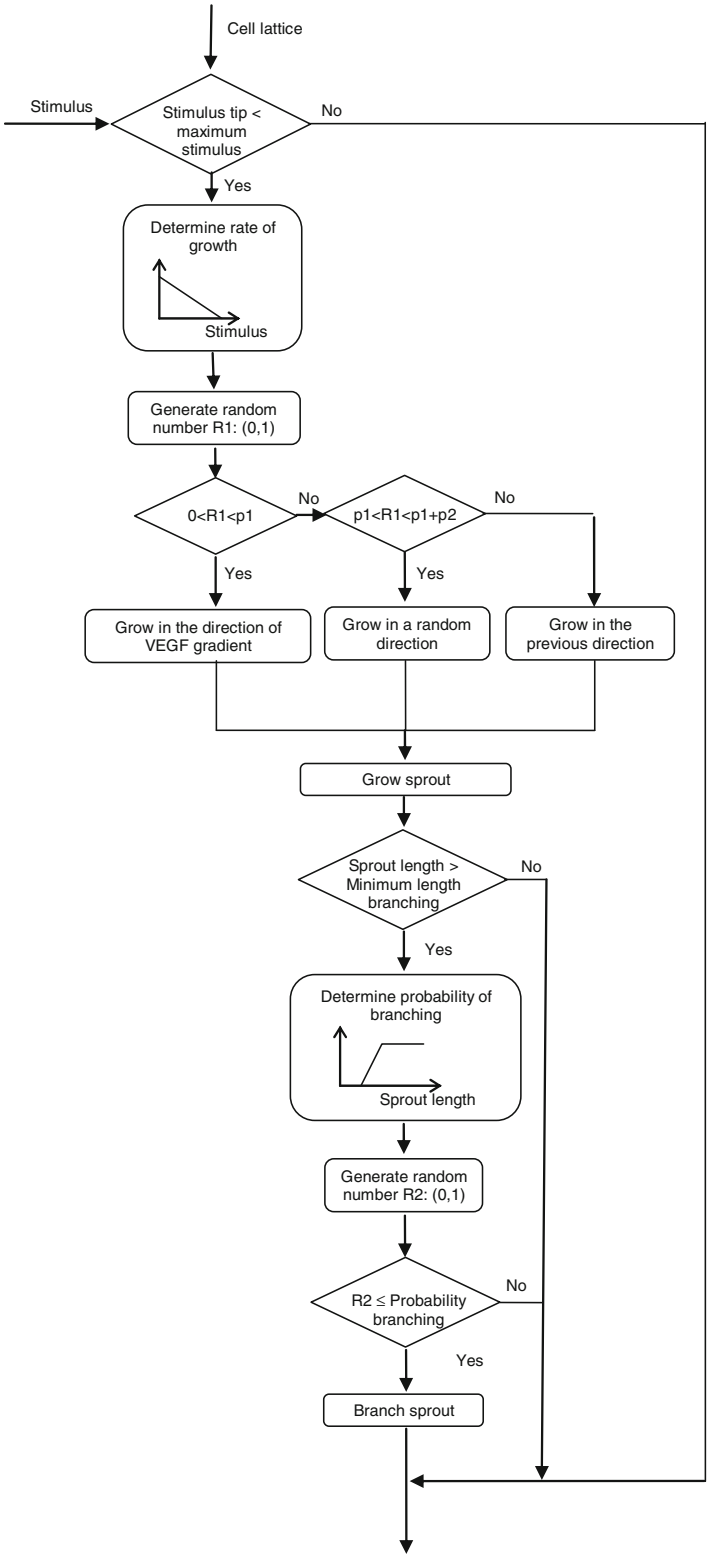

FIGURE 5. Flow chart diagram of computational algorithm to model angiogenesis.

assumed to apoptose at a rate of 30%. At the beginning of the simulation parent vessels were assumed to run at the interface between the bone and the gap tissue from which endothelial cells sprouted. In the simulations presented here, each iteration corresponds to a time increment of 1 day.

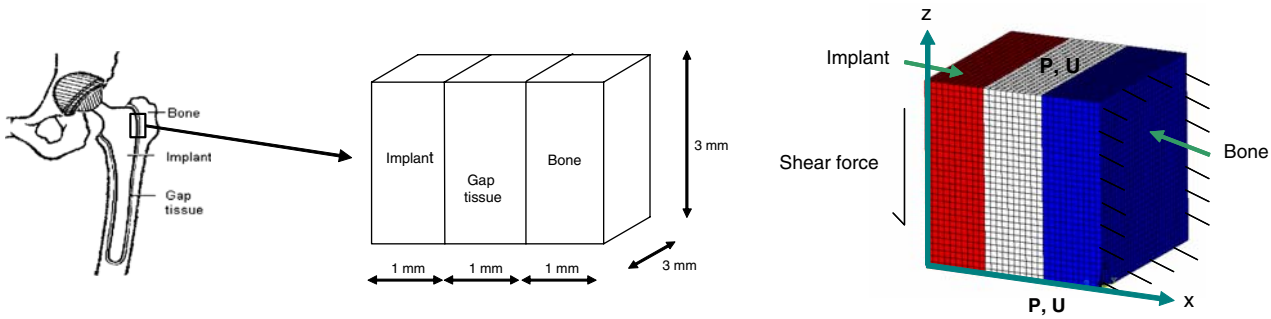

FIGURE 6. Finite element model of a bone/implant interface. A shear load is applied on the implant surface (i.e., $x = 0$) while the bone surface is constrained at $x = 3$ mm. Pore pressure (P) and nodal displacements (U) on the upper and lower surfaces (i.e., $z = 0$ and $z = 3$ mm) were imposed to be equal; this creates a boundary condition to approximate a repeating unit of a long implant *in situ*. The region may be thought as a piece of a cementless orthopedic implant fixation.

TABLE 1. Material properties.

	Granulation tissue	Fibrous tissue	Cartilage	Immature bone	Cortical bone
Young's modulus (MPa)	0.2	2[a]	10[b]	1,000	1,7000[c]
Permeability ($m^4/Ns \times 10^{-14}$)	1	1[a]	0.5[d]	0.1	0.001[e]
Poisson's ratio	0.167	0.167	0.3	0.3	0.3[e]
Bulk modulus grain (MPa)	2,300	2,300	3,700[f]	13,920	13,920[c]
Bulk modulus fluid (MPa)	2,300[g]	2,300[g]	2,300[g]	2,300[g]	2,300[g]

[a]Hori and Lewis[28]; [b]Claes and Heigele[16]; [c]Smit *et al.*[55]; [d]Armstrong and Mow[3]; [e]Cowin[19]; [f]Tepic *et al.*[59]; and [g]Anderson[1].

The simulations were performed using the finite element software Abaqus v6.6-1 together with user-developed subroutines in C.

Parametric Analysis

To identify the influence of various model parameters on the predictions, a statistical analysis of variance was used. A 2^5 factorial analysis with a single replicate[42,51] was performed to identify the effect of five vascularity-related parameters: minimum sprout length for branching (L_{min}), maximum length of a nonbranching sprout (L_{max}), maximum length increment per iteration (ΔL_{max}), maximum stimulus at the tip of a growing sprout (S_{max}), and oxygen diffusion distance ($L_{diffusion}$). Each of these parameters was represented at two levels (Table 2). Their effect on two output variables was analyzed:

- The number of endothelial cells per unit volume forming the newly developed vascularity at iteration 24 (i.e., 24 days)
- The number of bone-forming cells (osteoblasts) per unit volume at iteration 24.

In this implementation, p_1, p_2, and p_3 were considered 0.4, 0.4, and 0.2, respectively.

TABLE 2. Vascularity-related parameter at two different levels of the 2^5 factorial analysis.

Level	L_{min} (μm)	L_{max} (μm)	ΔL_{max} (μm/h)	S_{max}	$L_{diffusion}$ (μm)
Low	100[a]	300[a]	33[a,b]	3	100[c]
High	200[a]	500[a]	66[a,b]	5	200[c]

Underlined values correspond to the baseline simulation.
[a]Stokes and Lauffenburger[57]; [b]Kenyon *et al.*[37]; and [c]Carmeliet and Jain.[11]
$S_{max} = 3$: stimulus at the boundary between cartilage and fibrous tissue formation.
$S_{max} = 5$: stimulus for fibrous tissue formation.

RESULTS

The simulation predicted a capillary network with a realistic dentritic structure. Under a force-control situation, with a shear load to give an initial relative displacement between the bone and the implant of 117 μm, initially the high mechanical environment at the bone/tissue interface prevented the growth of the vessels. After a certain time and due to the tissue differentiation process, the degree of micromotion decreased, reducing the mechanical stimuli at the site, allowing the vessels to grow (Fig. 7). Under this loading condition, MSCs first differentiated into fibroblasts. As the repairing tissue started to stiffen, the

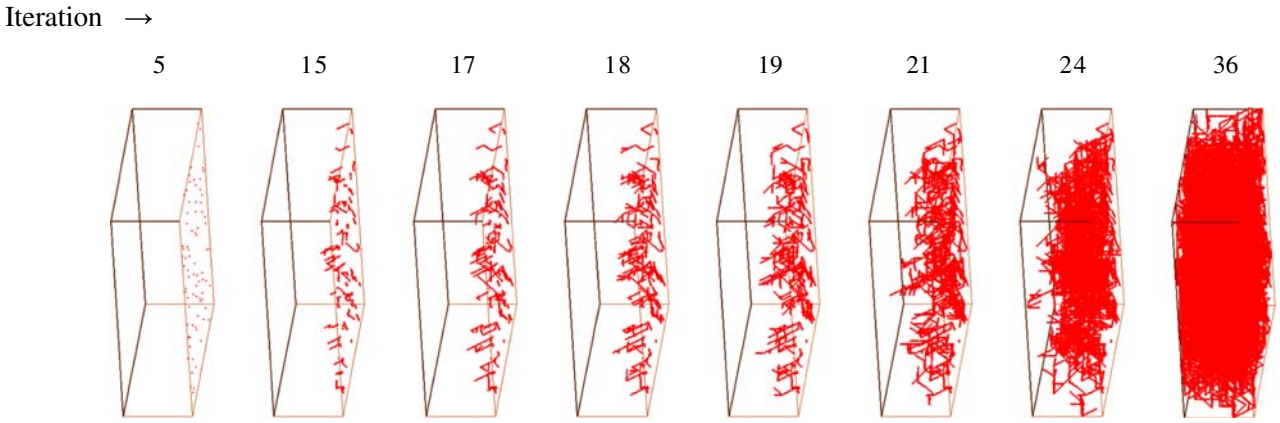

FIGURE 7. Capillary network formation in the regenerating tissue between the bone and the implant. Shear force to obtain an initial relative displacement between the bone and the implant of 117 μm.

mechanical stimulus decreased and chondrogenesis was favored. When the mechanical stimulus was sufficiently low, MSCs were predicted to differentiate into osteoblasts. By the time the osteogenic process started, blood vessels had not fully occupied the regenerating tissue and islands of osteoblasts were predicted surrounding the existing capillaries (Fig. 8).

The application of the higher shear load (to obtain an initial relative displacement between the bone and the implant of 233 μm) stopped vessels from growing until a later stage. Fibroblastic and chondrogenic differentiation of MSCs also occurred during longer periods of time with higher peaks in the concentration of fibroblasts and chondrocytes compared with the lower load case, 50% vs. 23% and 35% vs. 24%, respectively. Osteogenic differentiation started after vessels had developed for a longer period and, as a consequence, a faster and more uniform differentiation of MSCs into osteoblasts was observed (Fig. 9). By the end of the simulation (iteration 40), 29% of the positions were occupied by osteoblasts in the case of the higher load versus 32% in the case of the lower load.

Under displacement-control conditions, with a fixed relative displacement of 100 μm, a very poor vascular network developed and a fibrous tissue layer formed at the bone/implant interface, which remained throughout the simulation period (Fig. 10). After 40 days, endothelial cells only occupied 0.37% of the tissue volume. Under force-control conditions, at the same time point, the volume occupied by endothelial cells for the low and high load cases were 2.8% and 1.8%, respectively.

The model presented a nondeterministic behavior, especially in relation to cell distribution. Five simulations were performed using the baseline parameters (see Table 2) and simulation results were compared. No significant differences were observed in the reduction rate of the relative displacement between the bone and the implant; however, significantly different cell distribution patterns were predicted for each simulation (Fig. 11). In this respect, the simulation reproduces some of the variability observed in the experiments.

Oxygen diffusion distance had a significant influence on the rate of bone formation. Increasing the diffusion distance caused a more rapid formation of osteoblasts and an earlier apoptosis of chondrocytes (Fig. 12). By the end of the simulation, blood vessels were found distributed all along the regenerating tissue and therefore the number of osteoblasts was very similar independently of the oxygen diffusion distance. A maximum density of osteoblasts (about 35%) was predicted, independently of the oxygen diffusion distance, which corresponds to the cell density needed to reduce the mechanical environment in the regenerating tissue below the bone formation region and into bone resorption values. Once this density was reached, mesenchymal stem cells stopped differentiating into osteoblasts and equilibrium was reached. Endothelial cell density remained relatively low during the whole simulation period when compared to other cell phenotypes.

When an infinite diffusion distance was considered (equivalent to switching off the angiogenic rule in the tissue differentiation algorithm except from the fact that some cell positions were occupied by endothelial cells) a more spatially uniform distribution of the cells was predicted (Fig. 13a). Small differences were found in the reduction rate of the relative displacement between the bone and the implant (Fig. 13b).

The analysis of variance showed those factors which have a significant influence on the development of the new vasculature. The effect estimates showed that two factors, the maximum rate increase of a sprout (ΔL_{max}) and the maximum stimulus for a growing vessel (S_{max}) have large effects on endothelial cell density. Together they account for 80% of the variability in the number of endothelial cells per unit volume (Table 3). The other factors effects were small, with 7.4% coming

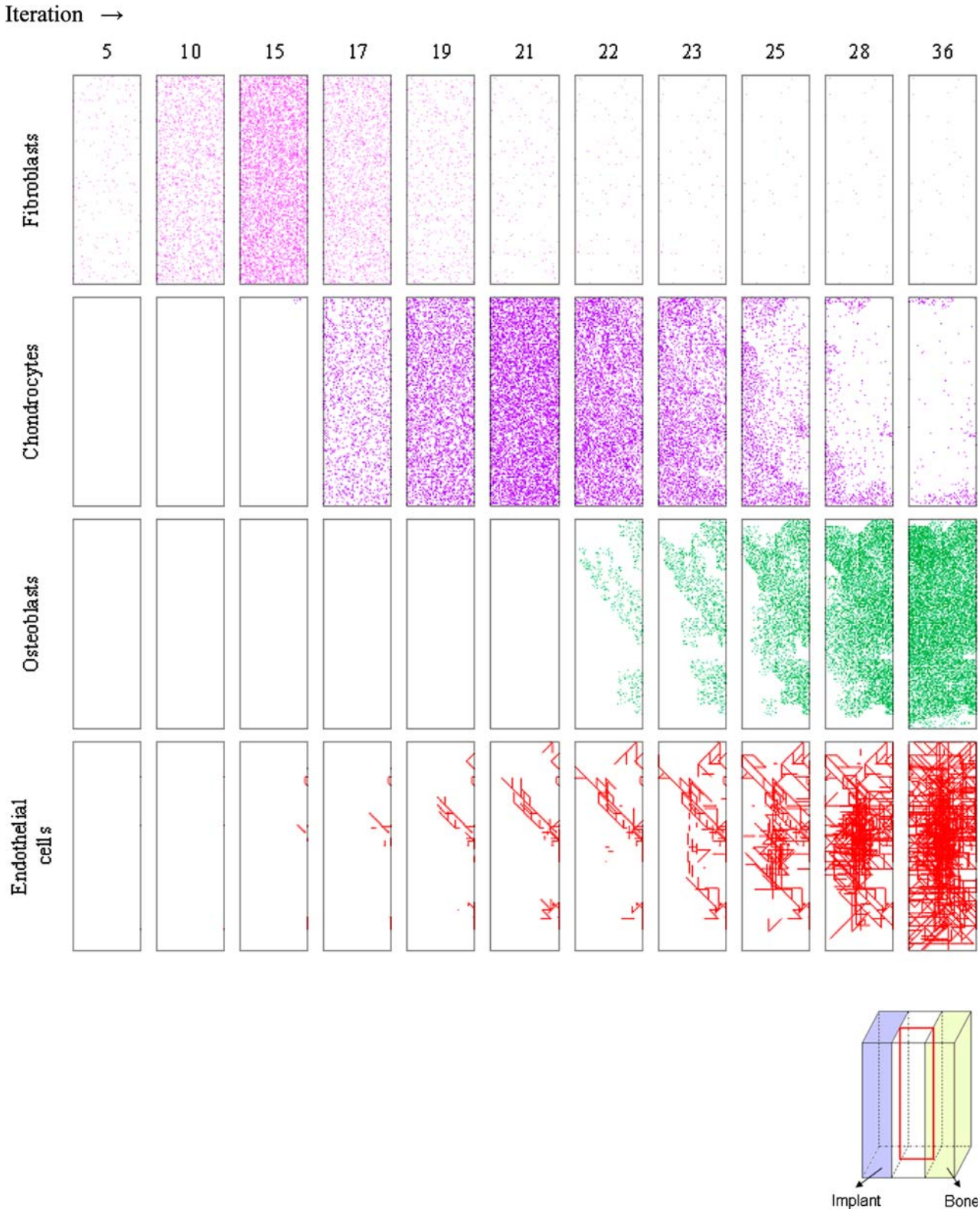

FIGURE 8. Distribution of the different cell phenotypes in a cross section through the middle of the regenerating tissue under force-control conditions (shear force to obtain an initial relative displacement between the bone and the implant of 117 μm). Endothelial cell distributions include all endothelial cells within 100 μm (oxygen diffusion distance) from the selected section. Each dot represents a cell occupying a lattice point.

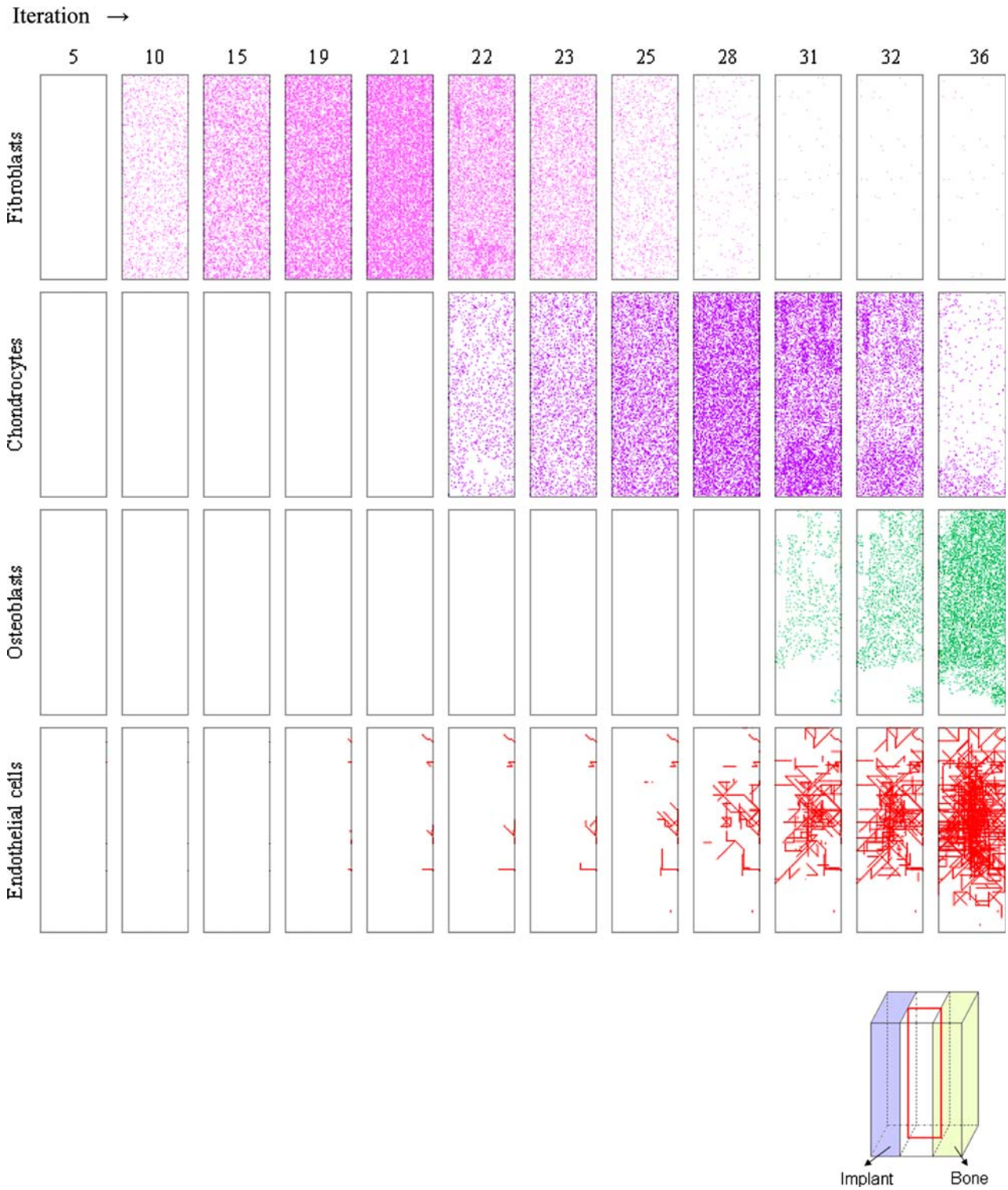

FIGURE 9. Distribution of the different cell phenotypes in a cross section through the middle of the regenerating tissue under force-control conditions (shear force to obtain an initial relative displacement between the bone and the implant of 233 μm). Endothelial cell distributions include all endothelial cells within 100 μm (oxygen diffusion distance) from the selected section. Each dot represents a cell occupying a lattice point.

from L_{max} and 8% coming from the interaction $\Delta L_{max} - S_{max}$. An increase in endothelial cell density was predicted when decreasing L_{max} or increasing ΔL_{max} and/or S_{max}. Three factors have large effect on osteoblast density: the maximum rate increase of a sprout (ΔL_{max}) with a 32.6% contribution to the total

FIGURE 10. Distribution of the different cell phenotypes in a cross section through the middle of the regenerating tissue under displacement-control conditions (relative displacement 100 μm). Endothelial cell distributions include all endothelial cells within 100 μm (oxygen diffusion distance) from the selected section. Each dot represents a cell occupying a lattice point.

variability, the maximum stimulus for a growing vessel (S_{max}) with 23%, and the oxygen diffusion distance ($L_{diffusion}$) with 23.8%. The maximum length of a nonbranching sprout (L_{max}) and the interactions $\Delta L_{max} - S_{max}$ and $\Delta L_{max} - S_{max} - L_{diffusion}$ had smaller effects, between 3% and 5%. An increase in the number of osteoblasts per unit volume was predicted when increasing L_{max}, ΔL_{max}, or S_{max}.

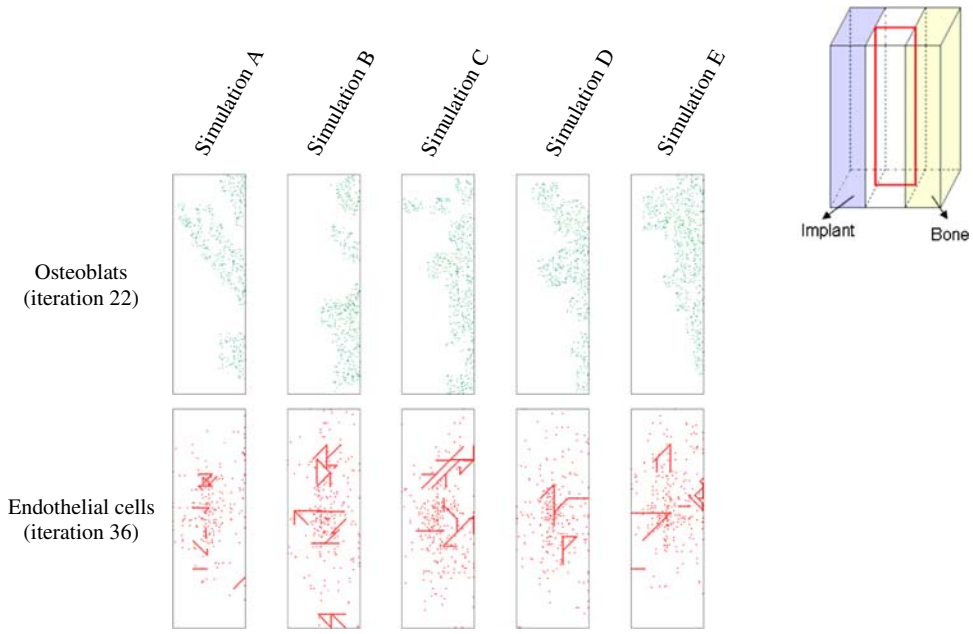

FIGURE 11. Osteoblast and endothelial cell distributions in a cross section through the middle of the regenerating tissue for five simulations (A, B, C, D, E) with the baseline parameters at iterations 22 and 36, respectively. Each dot represents a cell occupying a lattice point. The nondeterministic behavior of the model is shown by the differences in cell distribution patterns. Shear force to obtain an initial relative displacement between the bone and the implant of 117 μm.

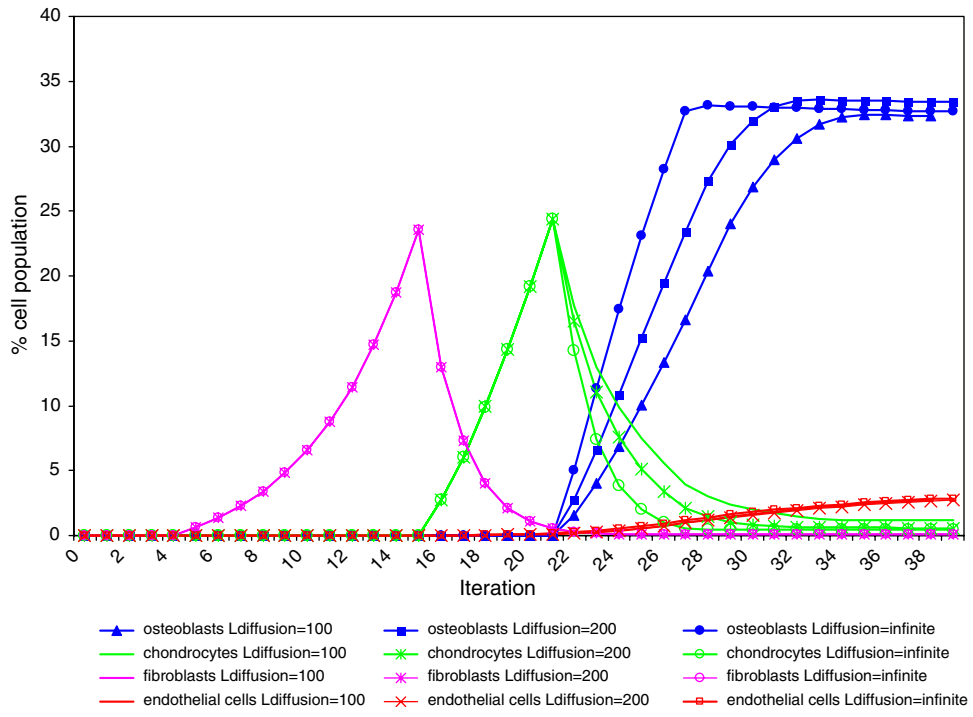

FIGURE 12. Percentage of cell positions occupied by fibroblasts, chondrocytes, osteoblasts, and endothelial cells for three different oxygen diffusion distances: 100 μm, 200 μm, and an infinite distance (equivalent to switching off the angiogenic rule in the tissue differentiation process but with endothelial cells occupying some of the cell positions). Shear force to obtain an initial relative displacement between the bone and the implant of 117 μm.

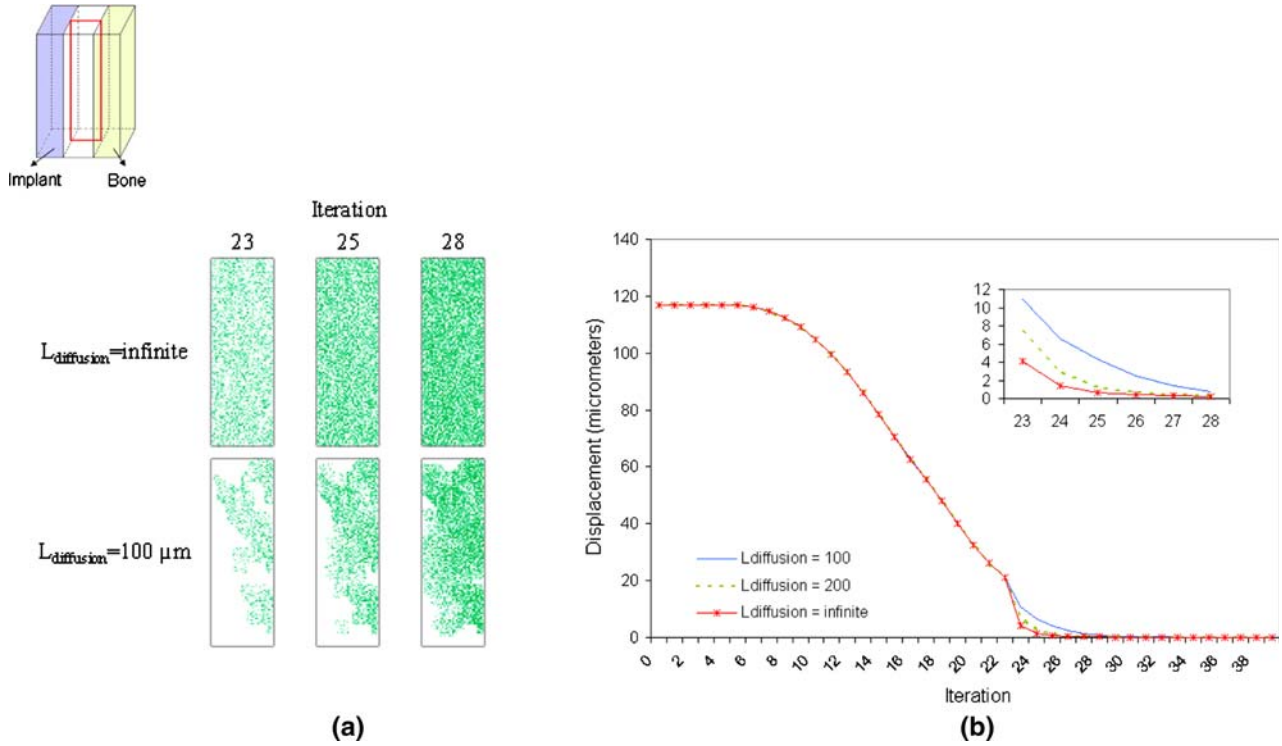

FIGURE 13. (a) Osteoblast distributions in a cross section through the middle of the regenerating tissue for oxygen diffusion distances of 100 μm and infinite. Each dot represents an osteoblast occupying a lattice point. (b) Displacement of the bone relative to the implant for oxygen diffusion distances of 100 μm, 200 μm, and infinite (equivalent to switching off the angiogenic rule in the tissue differentiation algorithm but with endothelial cells occupying some of the cell positions). Shear force to obtain an initial relative displacement between the bone and the implant of 117 μm.

TABLE 3. Contribution (%) of the main factors to the variability in the number of osteoblasts and endothelial cells per unit volume.

	Osteoblasts (%)	Endothelial cells (%)
L_{max}	5	7.4
ΔL_{max}	32.6	42.4
S_{max}	23	37.6
$L_{diffusion}$	23.8	–
$\Delta L_{max} - S_{max}$	3	8
$\Delta L_{max} - S_{max} - L_{diffusion}$	4	–

DISCUSSION

The computational model presented in this paper develops previous mechanoregulation simulations for tissue differentiation by including the vascular network development for the first time. This is possible because a lattice is employed within which cell activity can be simulated. Including capillary growth enables a explicit inclusion of the morphology of the new vasculature which may play a fundamental role during osteogenesis.[27,33] To evaluate the incorporation of capillary growth, and demonstrate the importance of the morphology of the new capillary network on tissue distributions, the model was also investigated by "turning off" the angiogenic process. Predictions corroborated our hypothesis that cell distribution and tissue differentiation patterns are significantly affected by capillary network formation. However, no great effect on force/displacement behavior of the regenerating tissue was predicted.

Although important aspects have been added in this model, it is still based on several simplifications. The process of capillary length increase, branching, and anastomosis are crucial for successful angiogenesis, but are not well quantified. The precise stimuli for vessel growth and branching are still unclear. Here we included a simple set of rules for length increase, branching, and looping. It is likely that more complex mechanisms are at work. For example, branching may be stimulated by high concentrations of growth factors; however, to date, the branching process has only been quantified in relation to vessel length. We believe the simple approach we have taken is the appropriate one given the information available and it highlights areas for future improvement.

The approach followed in this study to account for contact inhibition represents just one of the possible options. In the simulations presented here, cell proliferation would happen as far as there is a free space

surrounding the proliferating cell. This causes a fast increase in the number of cells, especially at the beginning, when MSCs are not mature enough to differentiate. Another possibility would be to inhibit cell proliferation if the first position chosen for the mitotic cells is occupied, i.e., not searching if there are neighboring free positions; this would make proliferation a slower process. Future investigations should be made on the effect of the dynamics of the proliferation process on tissue differentiation.

In addition, extracellular matrix production has been indirectly considered through the quantification of the associated cells. A proportional relation between number of cells and matrix production has been considered together with an immediate synthesis of extracellular matrix after cell differentiation. This is a simplification of the actual biology of the process that needs to be further developed in future versions of the model. For example, as previously proposed by Byrne *et al.*,[10] an exponential rate equation for the increase of tissue stiffness could be used to better match experimental observations.

Although there is experimental evidence supporting that cell migration, proliferation and apoptosis may be regulated by the mechanical environment,[34] in the simulations presented here, both processes are independent of the mechanical stimulus. However, it is clear that stimulus-dependent migration and proliferation could be easily implemented in future developments of the model.

Simulations were terminated when cell densities had reached an equilibrium. This happened when, due to stiffening of the regenerating tissue, the mechanical stimulus went below bone formation values and into the bone resorption region. This corresponds to the process known as bone remodeling, which was not included in the model. Similarly, in reality, newly formed microvessels would remodel spontaneously after a certain time, leading to pruning of the vascular network, a process which has not been included in the model.

Another aspect to take into account is the large number of parameters comprised in the model. Some of them have been directly obtained from experimental studies (cell diameter, oxygen diffusion distance, capillary rate of growth), some have been taken from previous computational models (initial mesenchymal stem cell concentration, differentiation rate, maturation age, migration and proliferation rates), and some have been merely estimated (maximum mechanical stimulus for blood vessel growth and apoptosis rate). The difficulty of finding adequate values for the parameters due to the lack of direct experimental measurements is a drawback of most computational models of this kind. In a recent study, Isaksson *et al.*[31] described, in a very thorough review, the experimental data available on some of these parameters showing that, in fact, several can be relatively well determined from available experimental literature. However, they are not drawn from a single experiment but from different experiments carried out under different conditions, on different animals, and on different parts of the skeleton. So the question is to what extent these values are representative of the tissue differentiation process in a completely different environment and if they can be applied to a population of individuals or if, in fact, high variability exists between different individuals and animals. Further research is needed to improve our understanding of the variability present on tissue differentiation processes.

In the simulation of angiogenesis, parameter values were, when possible, taken from experimental studies. The amount of oxygen required for cell survival has been reported to be limited to a distance of approximately 100–200 μm from the supplying blood vessel.[11,18] A baseline value for oxygen diffusion distance ($L_{\text{diffusion}}$) of 100 μm was considered in this study. Sholley *et al.*[54] measured 15 new branches connected to a pre-existing vessel of 0.88 mm in length during a three-day period of angiogenesis. It was proposed that half of these branches originated from the pre-existing vessel and another half was formed due to anastomosis of sprouts with the vessel.[57] Therefore, in average, there was a sprout forming every 120 μm in the pre-existing vessel. In the baseline simulations, the minimum length for a sprout to branch, L_{min}, and the maximum length of a nonbranching sprout, L_{max}, were considered 100 and 300 μm, respectively. Kenyon *et al.*[37] demonstrated that the front edge of vascular networks moves at a speed of about 15 μm/h in response to fibroblast growth factor stimulation in a mouse cornea pocket assay. In addition, it has been reported that endothelial cells migrate spontaneously *in vitro* at a speed of ~20 μm/h and that the migration speed is increased to 40 μm/h when endothelial cells are stimulated by acidic fibroblast growth factor.[57] Considering a maximum length increase of 200 μm every 6 h, the maximum rate of growth (ΔL_{max}) was about 33 μm/h; therefore, our value is within the range of experimentally measured values. To investigate the effect of several model parameters on the model response, a factorial analysis was performed. When selecting the size of the factorial design a compromise had to be sought between the number of chosen parameters, the number of levels, and computational cost. With this in mind, five vascularity-related model parameters were evaluated, each at two levels. Both vasculature network density and osteoblast density were influenced by the maximum stimuli and the maximum rate of growth. In addition, oxygen

diffusion distance had a significant effect on bone formation.

Despite limitations the model has successfully predicted many features of angiogenesis and the tissue differentiation process observed during experimental studies. It describes the overall dentritic structure and pattern of the capillary network similar to those observed *in vivo* (see for example, Lu *et al.*[41]). The experimental quantification of newly formed microvessels constitutes an active field of research[45,63] and not many quantitative studies have looked at angiogenesis during a bone regeneration process. Microvascular networks are difficult to quantify due to their small size, location, and complex 3D structure. Brey *et al.*[7] measured vascularity into a fibrin gel implanted against the skeletal muscle of rats. After 7 days, they measured endothelial cell densities of about 4.5% in the gel and 1.4% in the adjacent muscle bed. In a study by Moore *et al.*[43] measurements of vessel density were made during distraction osteogenesis of a rat femur. They found that vessels made up about 4% of the tissue volume at day 7 and by day 49 they were about 15%. Rai *et al.*[49] measured the vascular volume fraction after implantation of scaffolds into 8-mm rat nonunion femoral defects. Three weeks postimplantation they reported a vascular volume fraction of about 1%. In the simulations presented in this paper, capillary densities at the end of the simulations were 2.8% and 1.8% for the low and high load-control cases, respectively. Although values are of the same order of magnitude, microvascular networks exhibit wide variation in different physiological environments and anatomical locations and therefore the comparison is not sufficient to be considered a corroboration of the model.

Relatively uniform cell distributions were predicted when tissue differentiation was simulated without the angiogenesis algorithm; however, when angiogenesis was incorporated in the algorithm heterogeneous distributions of cells were found. These results show some similarity with histological observations of osseointegration in that clusters of cells appear (see for example, Götz *et al.*[24]). Noncontinuous distributions of cells were previously reported by Pérez and Prendergast[48] when using a random walk model for the simulation of cell dispersal. In that study, as in the simulations presented here where angiogenesis was 'turned off,' the irregularity in the distribution of cells was very subtle and it did not predict rapid changes of cell density within the regenerating tissue as those seen in histological studies[24]; therefore, we would conclude that the random nature of cell migration/proliferation causes heterogeneous cell distributions but that angiogenesis further develops it. Previously, Geris *et al.*[23] used a continuum modeling approach to take account of the angiogenic process in a tissue differentiation algorithm applied to fracture healing, with the main limitation of not considering the effect of the mechanical environment. Using diffusion equations to model the dispersal of cells, they described the spatiotemporal change of the density of different cell populations in the regenerating tissue. In the model presented here, individual cell activity is taken into account using a lattice model, which allows for the simulation of the highly structured pattern in which endothelial cells organize when forming new capillaries.

In conclusion, bone formation (and more generally tissue differentiation) patterns have been predicted to be influenced by capillary network formation. The model will have to be further tested by attempting to simulate tissue differentiation in different circumstances; nonetheless, initial results suggest that it can predict the coupling between angiogenesis and tissue differentiation, and could be used as an investigational tool in tissue repair and tissue engineering research.

ACKNOWLEDGMENTS

This work was supported by the European Commission, Sixth Framework Programme Priority, SmartCap, and Science Foundation Ireland.

REFERENCES

[1]Anderson, C. B. Mechanics of fluids. In: Marks's Standard Handbook of Mechanical Engineers, edited by Y. Baumesiter. New York: McGraw-Hill, 2006, pp. 3.48–3.76.

[2]Andreykiv, A., F. van Keulen, and P. J. Prendergast. Simulation of fracture healing incorporating mechanoregulation of tissue differentiation and dispersal/proliferation of cells. *Biomech. Model. Mechanobiol.* 7:443–461, 2008.

[3]Armstrong, C. G., and V. C. Mow. Variations in the intrinsic mechanical properties of human articular cartilage with age, degeneration and water content. *J. Bone Joint Surg. Am.* 64:88–94, 1982.

[4]Aspenberg, P., S. Goodman, S. Toksvig-Larsen, L. Ryd, and T. Albrektsson. Intermittent micromotion inhibits bone ingrowth. Titanium implants in rabbits. *Acta Orthop. Scand.* 63:141–145, 1992.

[5]Blenman, P. R., D. R. Carter, and G. S. Beaupre. Role of mechanical loading in the progressive ossification of a fracture callus. *J. Orthop. Res.* 7:398–407, 1989. doi:10.1002/jor.1100070312.

[6]Branemark, P. I. Osseointegration and its experimental background. *J. Prosthet. Dent.* 50:399–410, 1983. doi:10.1016/S0022-3913(83)80101-2.

[7]Brey, E. M., T. W. King, C. Johnston, L. V. McIntire, G. P. Reece, and C. W. Patrick. A technique for quantitative three-dimensional analysis of microvascular structure.

Microvasc. Res. 63:279–264, 2002. doi:10.1006/mvre.2002.2395.

[8]Brunski, J. B. In vivo bone response to biomechanical loading at the bone/dental-implant interface. *Adv. Dent. Res.* 13:99–119, 1999.

[9]Burke, D. W., D. O. O'Connor, E. B. Zalenski, M. Jasty, and W. H. Harris. Micromotion of cemented and uncemented femoral components. *J. Bone Joint Surg.* 73B:33–37, 1991.

[10]Byrne, D. P., D. Lacroix, J. A. Planell, D. J. Kelly, and P. J. Prendergast. Simulation of tissue differentiation in a scaffold as a function of porosity, Young's modulus and dissolution rate: application of mechanobiological models in tissue engineering. *Biomaterials* 28:5544–5554, 2007. doi:10.1016/j.biomaterials.2007.09.003.

[11]Carmeliet, P., and M. K. Jain. Angiogenesis in cancer and other diseases. *Nature* 407:249–257, 2000. doi:10.1038/35025220.

[12]Carter, D. R., P. R. Blenman, and G. S. Beaupre. Correlations between mechanical stress history and tissue differentiation in initial fracture healing. *J. Orthop. Res.* 7:398–407, 1988.

[13]Cenni, E. Angiogenesis and bone regeneration. *J. Bone Joint Surg.* 87B:58, 2005.

[14]Claes, L., K. Eckert-Hubner, and P. Augat. The effect of mechanical stability on local vascularisation and tissue differentiation in callus healing. *J. Orthop. Res.* 20:1099–1105, 2002. doi:10.1016/S0736-0266(02)00044-X.

[15]Claes, L., K. Eckert-Hubner, and P. Augat. The fracture gap size influences the local vascularisation and tissue differentiation in callus healing. *Langenbecks Arch. Surg.* 388:316–322, 2003. doi:10.1007/s00423-003-0396-0.

[16]Claes, L. E., and C. A. Heigele. Magnitudes of local stress and strain along bony surfaces predict the course and type of fracture healing. *J. Biomech.* 32:255–266, 1999. doi:10.1016/S0021-9290(98)00153-5.

[17]Colnot, C., Z. Thompson, T. Miclau, Z. Werb, and J. A. Helms. Altered fracture repair in the absence of MMP9. *Development* 130:4123–4133, 2003. doi:10.1242/dev.00559.

[18]Colton, C. K. Implantable biohybrid artificial organs. *Cell Transplant.* 4:415, 1995. doi:10.1016/0963-6897(95)00025-S.

[19]Cowin, S. C. Bone poroelasticity. *J. Biomech.* 32:217–238, 1999. doi:10.1016/S0021-9290(98)00161-4.

[20]Eckardt, H., M. Ding, M. Lind, E. S. Hansen, K. S. Cristensen, and I. Hvid. Recombinant human vascular endothelial growth factor enhances bone healing in an experimental non-union model. *J. Bone Joint Surg. Br.* 87:1434–1438, 2005. doi:10.1302/0301-620X.87B10.16226.

[21]Gerber, H. P., T. H. Vu, A. M. Ryan, J. Kowalski, Z. Werb, and N. Ferrara. VEGF couples hypertrophic cartilage remodelling, ossification and angiogenesis during endochondral bone formation. *Nat. Med.* 5:623–628, 1999. doi:10.1038/9467.

[22]Geris, L., A. Andreykiv, H. Van Oosterwyck, J. V. Sloten, F. van Keulen, J. Duyck, and I. Naert. Numerical simulation of tissue differentiation around loaded titanium implants in a bone chamber. *J. Biomech.* 37:763–769, 2004. doi:10.1016/j.jbiomech.2003.09.026.

[23]Geris, L., A. Gerisch, J. V. Stolen, R. Weiner, and H. V. Oosterwyck. Angiogenesis in bone fracture healing: a bioregulatory model. *J. Theor. Biol.* 251:137–158, 2007. doi:10.1016/j.jtbi.2007.11.008.

[24]Götz, H. E., M. Müller, A. Emmel, U. Holzwarth, R. G. Erben, and R. Stangl. Effect of surface finish on the osseointegration of laser-treated titanium alloy implants. *Biomaterials* 25:4057–4064, 2004. doi:10.1016/j.biomaterials.2003.11.002.

[25]Haller, A. Experimentorum de ossiem formatione. In: Opera minora. Laussanne: Francisci Grasset, 1763, p. 400.

[26]Hausman, M. R., M. B. Schaffler, and R. J. Majesta. Prevention of fracture healing in rats by an inhibitor of angiogenesis. *Bone* 29:560–564, 2001. doi:10.1016/S8756-3282(01)00608-1.

[27]Hirao, M., N. Tamai, N. Tsumaki, H. Yoshikawa, and A. Myoui. Oxygen tension regulates chondrocyte differentiation and function during endochondral ossification. *J. Biol. Chem.* 281:31079–31092, 2006. doi:10.1074/jbc.M602296200.

[28]Hori, R. Y., and J. L. Lewis. Mechanical properties of the fibrous tissue found at the bone-cement interface following total joint replacement. *J. Biomed. Mater. Res.* 16:911–927, 1982. doi:10.1002/jbm.820160615.

[29]Huiskes, R., W. D. Van Driel, P. J. Prendergast, and K. Søballe. A biomechanical regulatory model for peri-prosthetic fibrous tissue differentiation. *J. Mater. Sci.: Mater. Med.* 8:785–788, 1997. doi:10.1023/A:1018520914512.

[30]Isaksson, H., O. Comas, C. C. van Donkelaar, J. Mediavilla, W. Wilson, R. Huiskes, and K. Ito. Bone regeneration during distraction osteogenesis: mechano-regulation by shear strain and fluid velocity. *J. Biomech.* 40:2002–2011, 2006. doi:10.1016/j.jbiomech.2006.09.028.

[31]Isaksson, H., C. C. van Donkelaar, R. Huiskes, and K. Ito. A mechano-regulatory bone-healing model incorporating cell-phenotype specific activity. *J. Theor. Biol.* 21:230–246, 2008. doi:10.1016/j.jtbi.2008.01.030.

[32]Isaksson, H., W. Wilson, C. C. van Donkellaar, R. Huiskes, and K. Ito. Comparison of biophysical stimuli for mechano-regulation of tissue differentiation during fracture healing. *J. Biomech.* 39:1507–1516, 2006. doi:10.1016/j.jbiomech.2005.01.037.

[33]Kanichai, M., D. Ferguson, P. J. Prendergast, and V. A. Campbell. Hypoxia promotes chondrogenesis in rat mesenchymal stem cells: a role for AKT and Hypoxia-Inducible Factor (HIF)-1α. *J. Cell. Physiol.* 216:708–715, 2008.

[34]Kearney, E. M., P. J. Prendergast, and V. A. Campbell. Mechanisms of strain-mediated mesenchymal stem cell apoptosis. *J. Biomech. Eng.* 130:061004, 2008.

[35]Kelly, D. J., and P. J. Prendergast. Mechano-regulation of stem cell differentiation and tissue regeneration in osteochondral defects. *J. Biomech.* 38:1413–1422, 2005. doi:10.1016/j.jbiomech.2004.06.026.

[36]Kelly, D. J., and P. J. Prendergast. Prediction of optimal mechanical properties for a scaffold used in osteochondral defect repair. *Tissue Eng.* 12:2509–2519, 2006. doi:10.1089/ten.2006.12.2509.

[37]Kenyon, B. M., E. E. Voest, C. C. Chen, E. Flynn, J. Folkman, and R. J. D'Amato. A model of angiogenesis in the mouse cornea. *Invest. Ophthalmol. Vis. Sci.* 37:1625–1632, 1996.

[38]Lacroix, D., and P. J. Prendergast. A mechano-regulation model for tissue differentiation during fracture healing: analysis of gap size and loading. *J. Biomech.* 35:1163–1171, 2002. doi:10.1016/S0021-9290(02)00086-6.

[39]Lanza, R., E. D. Thomas, J. Thomson, and R. Pedersen. Essentials of Stem Cell Biology. New York: Academic Press, 2005.

[40]Liu, X., and G. L. Niebur. Bone ingrowth into a porous coated implant predicted by a mechano-regulatory tissue differentiation algorithm. *Biomech. Model. Mechanobiol.* 7:335–344, 2008.

[41]Lu, C., R. Marcucio, and T. Miclau. Assessing angiogenesis during fracture healing. *Iowa Orthop. J.* 26:17–26, 2006.
[42]Montgomery, D. C., and G. C. Runger. Applied Statistics and Probability for Engineers. 4th ed. New York: John Wiley & Sons, 2006.
[43]Moore, D. C., C. W. Leblanc, R. Müller, J. J. Crisco, III, and M. G. Ehrlich. Physiologic weight-bearing increases new vessel formation during distraction osteogenesis: a micro-tomographic imaging study. *J. Orthop. Res.* 21:489–496, 2003. doi:10.1016/S0736-0266(02)00234-6.
[44]Morgan, E. F., M. T. Longaker, and D. R. Carter. Relationships between tissue dilatation and differentiation in distraction osteogenesis. *Matrix Biol.* 25(2):94–103, 2006. doi:10.1016/j.matbio.2005.10.006.
[45]Norrby, K. Microvascular density in terms of number and length of microvessel segments per unit tissue volume in mammalian angiogenesis. *Microvasc. Res.* 55:43–53, 1998. doi:10.1006/mvre.1997.2054.
[46]Prendergast, P. J., R. Huiskes, and K. Søballe. Biophysical stimuli on cells during tissue differentiation at implants interfaces. *J. Biomech.* 30:539–548, 1997. doi:10.1016/S0021-9290(96)00140-6.
[47]Prendergast, P. J., and M. C. H. van der Meulen. Mechanics of bone regeneration. In: Bone Mechanics Handbook, edited by S. C. Cowin. Boca Raton, FL: CRC Press LCC, 2001, pp. 321–3213.
[48]Pérez, M., and P. J. Prendergast. Random-walk model of cell-dispersal included in mechanobiological simulation of tissue differentiation. *J. Biomech.* 40:2244–2253, 2007. doi:10.1016/j.jbiomech.2006.10.020.
[49]Rai, B., M. E. Oest, K. M. Dupont, K. H. Ho, S. H. Teoh, and R. E. Guldberg. Combination of platelet-rich plasma with plycaprolactone-tricalcium phosphate scaffolds for segmental bone repair. *J. Biomed. Mater. Res.* 81:888, 2007. doi:10.1002/jbm.a.31142.
[50]Rossi, F., H. E. MacLean, W. Yuan, R. O. Francis, E. Semenova, C. S. Lin, H. M. Kronenberg, and D. Cobrinik. p107 and p130 co-ordinately regulate proliferation, Cbfa1 expression, and hypertrophic differentiation during endochondral bone development. *Dev. Biol.* 247:271–285, 2002. doi:10.1006/dbio.2002.0691.
[51]Ruan, J., and P. Prasad. The influence of human head tissue properties on intracranial pressure response during direct head impact. *Int. J. Veh. Saf.* 1:282–291, 2006.
[52]Schenk, R. K., and D. Buser. Osseointegration: a reality. *Periodontology 2000* 7:22–35, 1998. doi:10.1111/j.1600-0757.1998.tb00120.x.
[53]Shefelbine, S. J., P. Augat, L. Claes, and U. Simon. Trabecular bone fracture healing simulation with finite element analysis and fuzzy logic. *J. Biomech.* 38:2440–2450, 2005. doi:10.1016/j.jbiomech.2004.10.019.
[54]Sholley, M. M., G. P. Ferguson, H. R. Seibel, J. L. Montour, and J. D. Wilson. Mechanisms of neovascularisation: vascular sprouting can occur without proliferation of endothelial cells. *Lab. Invest.* 51:624–634, 1984.
[55]Smit, T. H., J. M. Huyghe, and S. C. Cowin. Estimation of the poroelastic parameters of cortical bone. *J. Biomech.* 35:829–835, 2002. doi:10.1016/S0021-9290(02)00021-0.
[56]Smith-Adaline, E. A., S. K. Volkman, M. A. Ignelzi, Jr., J. Slade, S. Platte, and S. A. Goldstein. Mechanical environment alters tissue formation patterns during fracture healing. *J. Orthop. Res.* 22:1079–1085, 2004. doi:10.1016/j.orthres.2004.02.007.
[57]Stokes, C. L., and D. A. Lauffenburger. Migration of individual microvessel endothelial cells: stochastic model and parameter measurement. *J. Cell Sci.* 99:419–430, 1991.
[58]Szmukler-Moncler, S., H. Salama, Y. Reingewirtz, and J. H. Dubruille. Timing of loading and effect of micromotion on bone-dental implant interface: review of experimental literature. *J. Biomed. Mater. Res.* 43:192–203, 1998. doi:10.1002/(SICI)1097-4636(199822)43:2<192::AID-JBM14>3.0.CO;2-K.
[59]Tepic, S., T. Macirowski, and R. W. Mann. Mechanical properties of articular cartilage elucidated by osmotic loading and ultrasound. *Proc. Natl. Acad. Sci. USA* 80:3331–3333, 1983. doi:10.1073/pnas.80.11.3331.
[60]Terranova, V. P., R. Diflorio, R. M. Lyall, S. Hic, R. Friesel, and T. Maciag. Human endothelial cells are chemotactic to endothelial cell growth factor and heparin. *J. Cell Sci.* 101:2330–2334, 1985.
[61]Trueta, J. The role of the vessels in osteogenesis. *J. Bone Joint Surg.* 45B:402–418, 1963.
[62]Wallace, A. L., E. R. Draper, R. K. Strachan, I. D. McCarthy, and S. P. Hughes. The vascular response to fracture micromovement. *Clin. Orthop.* 301:281–290, 1994.
[63]Young, S., J. D. Kretlow, C. Nguyen, A. G. Bashoura, L. S. Baggett, J. A. Jansen, M. Wong, and A. G. Mikos. Microcomputed tomography characterization of neovascularisation in bone tissue engineering applications. *Tissue Eng.* 14:295–306, 2008.